Vibrational distributions of $N_2O^+(\tilde{A}\,^2\Sigma^+)$ produced by electron impact on jet-cooled N_2O

Ikuo Tokue, Mikio Kobayashi, and Yoshio Ito
Department of Chemistry, Faculty of Science, Niigata University, Ikarashi, Niigata 950-21, Japan

(Received 22 July 1991; accepted 27 January 1992)

Fluorescence spectra of the $N_2O^+(\tilde{A}\,^2\Sigma^+-\tilde{X}\,^2\Pi_i)$ system produced by electron impact on N_2O have been studied in the impact energy range of 22–100 eV in order to determine vibrational-state distributions of the $N_2O^+(\tilde{A}\,^2\Sigma^+)$ state. Emission bands from the 0^0, 2^1K^1, 2^2K^0, 1^1, 1^2, and 3^1 levels have been assigned. The populations of the 1^1 and 1^2 levels corrected for effects of predissociation are similar to those obtained by the threshold photoelectron method. It is concluded that these results are affected by autoionization via the Rydberg states converging to the $\tilde{C}\,^2\Sigma^+$ ion state. The population of the 2^1K^1 level is enhanced remarkably more than in photoionization data. This enhancement indicates that, in the electron impact, transitions with $\Delta K = \pm 1$ are allowed in the formation of $\tilde{A}\,^2\Sigma^+$.

I. INTRODUCTION

Formation of $N_2O^+(\tilde{A}\,^2\Sigma^+)$ by electron impact on N_2O was studied by several research groups.[1–3] These studies mainly pay attention to either absolute emission cross sections for the $N_2O^+(\tilde{A}\,^2\Sigma^+-\tilde{X}\,^2\Pi_i)$ system or fluorescence lifetimes of vibrational levels of the $\tilde{A}$ state. Nevertheless, vibrational-state distributions of $N_2O^+(\tilde{A})$ derived from the observed emission cross sections seem to be inadequate for discussion of ionization dynamics.

As for photoionization of N_2O, the vibrational distributions of $N_2O^+(\tilde{A})$ have been studied by photoelectron spectroscopy (PES)[4–6] and fluorescence spectroscopy.[7,8] However, the PES results[4,6] do not seem to be all consistent with the results obtained from threshold photoelectron spectroscopy (TPES).[5] Later, experimental[9,10] and theoretical[11,12] studies in photoionization of N_2O have provided semiquantitative insight into the ionization dynamics for formation of $N_2O^+(\tilde{A})$.[13] From vibrationally resolved spectroscopy of the $N_2O^+(\tilde{A}, v'-\tilde{X}, v'')$ fluorescence, Poliakoff *et al.*[7,8] determined vibrational branching ratios of the $v'=1^1$ and 3^1 levels relative to the 0^0 level of the $\tilde{A}$ state in the 16.4–22.5 eV range. These branching ratio curves clearly show many sharp autoionization peaks existing below 20.1 eV (the $\tilde{C}\,^2\Sigma^+$ threshold)[4] and a wing of a σ shape resonance.[11] Later, Kelly *et al.*[9] have provided a more complete analysis of the broad shape resonant structure by covering a wider energy range: The branching ratio for the 1^1 level strongly depends on the excitation energy, whereas that for the 3^1 level is essentially constant. These trends have been attributed to the shape resonance in the $7\sigma\rightarrow\epsilon\sigma$ photoionization channel.[11,12] Ferrett *et al.*[10] have studied vibrationally resolved photoelectron spectra of the 0^0, 1^1, 1^2, and 3^1 levels of the $\tilde{A}$ state in the 17.4–26 eV range. Their results of the vibrational branching ratios agree very well with the trends measured by Kelly *et al.*[8] In a previous study,[14] we have reported similar trends in the vibrational branching ratios for the 1^1 and 3^1 levels relative to the 0^0 level of the $N_2O^+(\tilde{A})$ state produced by electron impact on N_2O.

When a molecule is ionized by electron impact, several ion states below the impact energy can be excited via the optically allowed or forbidden transition; in other words, various types of excitation generally contribute to the formation of the specific ion state at a given impact energy since electron collisions are an energy-loss process in contrast to photoionization. Moreover, internal populations of the product ions can be affected by post-collision interactions with the scattered and ejected electrons especially near the ionization threshold. Accordingly, the dependence of the rovibrational distribution in the ion state of interest upon the impact energy should reflect the nature of excitation mechanism and ionization dynamics involved. In the present study, we report the vibrational distributions, $N(v')$, of $N_2O^+(\tilde{A}, v')$ produced by electron-impact ionization of N_2O. The $N(v')$ values were evaluated from the intensity ratios of the corresponding vibrational bands of the $\tilde{A}$–$\tilde{X}$ fluorescence. A pulsed supersonic free jet obtained from pure N_2O gas was subjected to the electron-impact ionization. Since the ions thus produced nearly retain the low rotational temperature of the parent neutrals,[15] the fluorescence spectrum from the ions is simplified. This enables us to analyze intensities of the vibronic bands unambiguously. After comparing our results with published data and calculated Franck–Condon factors, we discuss ionization dynamics in the collision of electrons with N_2O molecules.

II. EXPERIMENT

The experimental details were essentially the same as those reported elsewhere.[14,16] In brief, neat N_2O at a stagnation pressure of 280 Torr was expanded into the collision chamber through a nozzle (0.4 mm diam) pulsed at a repetition frequency of 5 Hz. An ambient pressure of the collision chamber was kept at 3×10^{-4} Torr and the electron beam source was evacuated to 2×10^{-5} Torr under operating conditions. The free jet crossed an electron beam perpendicularly about 1.5 cm down stream from the nozzle. The impact energy was calibrated against the appearance potential of the $N_2O^+(\tilde{A}$–$\tilde{X})$ emission (16.4 eV).[4] The energy spread in the electron beam was estimated to be about 1 eV (FWHM)

 0021-9606/92/107458-07$06.00

from the profile near the onset appeared in the excitation function for the 0_0^0 band.

Emission spectra of the N_2O^+ ($\tilde{A}$–$\tilde{X}$) transition were measured at a resolution of 0.06 nm or better. In the measurement, emissions produced by electron impact on ambient thermal N_2O molecules near the beam center were also detected. In order to eliminate the fluorescence from the thermalized N_2O^+ ($\tilde{A}$), the light intensity obtained at the nozzle-off period was subtracted from that obtained at the nozzle-on period. The relative intensity response of the monochromator and the detection system was calibrated with a standard halogen lamp.

III. RESULTS

A. Emission spectra of the $\tilde{A}\,^2\Sigma^+$–$\tilde{X}\,^2\Pi_i$ transition

Figure 1 shows a fluorescence spectrum of the N_2O^+ ($\tilde{A}$–$\tilde{X}$) system in the 335–422 nm region produced by electron impact on jet-cooled N_2O at 100 eV. Vibrational bands were assigned with the aid of the table of Callomon and Creutzberg.[17] To describe the spectrum, we have followed their notation: the symbol K, which is given in the transitions for bending vibration (ν_2), means the vibronic angular momentum about the internuclear axis ($K = \Lambda + 1$), where $\Lambda(h/2\pi)$ and $l(h/2\pi)$ represent the electronic and vibrational angular momentum, respectively, about the internuclear axis. Many vibrational bands consist of a pair of subbands with almost equal intensity owing to the spin–orbit splitting of the $\tilde{X}\,^2\Pi$ state.[17] Each of the subbands is single headed, whereas that obtained by Penning ionization of N_2O in a flowing helium afterglow is double headed.[18] This difference mainly originates in the rotational cooling of target molecules in a supersonic jet. The rotational state distributions for the 0^0 level of the $\tilde{A}$ state produced at an impact energy of 100 eV have been nearly represented by an effective temperature of 23 K.[15] Such a low temperature enables us to assign the vibrational bands easily and to analyze the intensity of each vibrational band unambiguously.

The vibrational bands displayed in Fig. 1 are grouped into six series; vibrational bands in each series have the same upper level. Emissions from the 0^0, 1^1, and 3^1 levels of the $\tilde{A}$ state are prominent, while weaker bands from the 1^2, 2^1K^1, and 2^2K^0 levels are also observed. From the photoelectron–photoion coincidence measurement, Eland[19] concluded that N_2O^+ ions in the 0^0 level of the $\tilde{A}$ state all fluoresce, whereas those in the vibrationally excited levels predissociate. No emission from the $1^12^1K^1$, 1^13^1, and 3^2 levels which were identified in HeI PES[4,6] was observed in the present study. This result together with the weakness of the emissions from the 1^2 level is probably attributed to predissociation.

B. Vibrational populations of the $\tilde{A}\,^2\Sigma^+$ state

When the efficiency of the fluorescence detecting system was corrected, the emission intensity $I(v', v'')$ in photon/s for the N_2O^+ ($\tilde{A}$, $v' - \tilde{X}$, v'') transition can be represented by the r-centroid approximation as follows:[20]

$$I(v',v'') \propto N(v')\cdot\Phi_F(v')\cdot\nu(v',v'')^3\cdot q(v',v'')\cdot R_e(\bar{r}_{v'v''})^2, \tag{1}$$

where $q(v', v'')$ and $\nu(v', v'')$ are the Franck–Condon factor (FCF) and the transition frequency, respectively, for the v'–v'' band. The $N(v')$ and $\Phi_F(v')$ represent the vibrational population and the fluorescence quantum yield, respectively, for the v' level produced by electron impact; hence, Φ_F represents fluorescence versus dissociation branching ratio since fluorescence from vibrationally excited levels of the $\tilde{A}$ state is known to compete with predissociation.[19] Although the electronic transition moment $R_e(\bar{r}_{v'v''})$ generally depends on the internuclear distance, there is very little quanti-

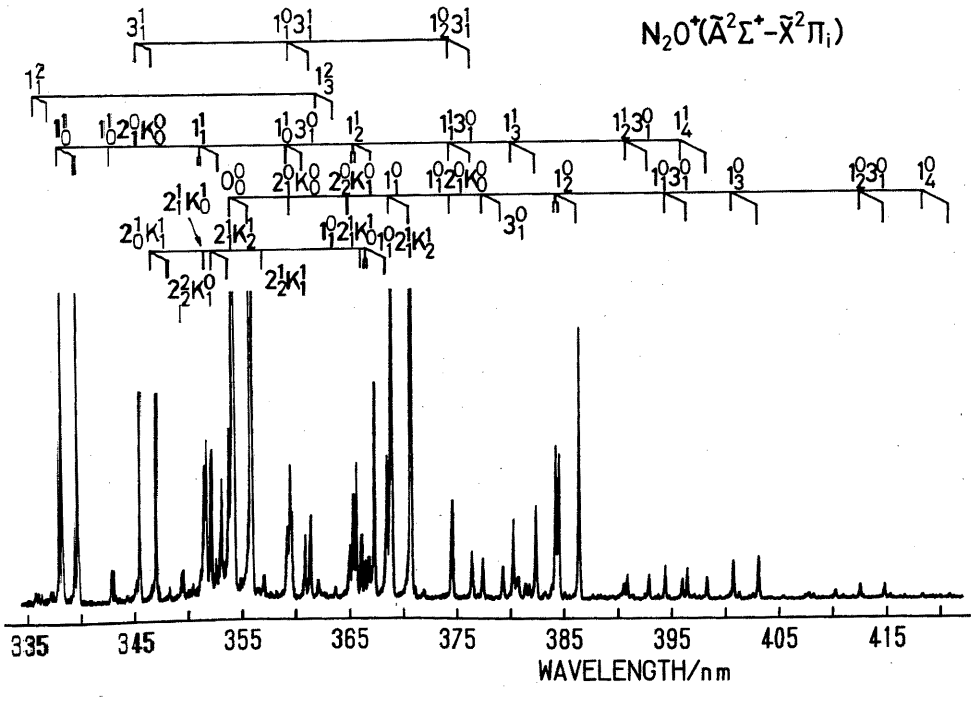

FIG. 1. Fluorescence spectrum of the N_2O^+ ($\tilde{A}\,^2\Sigma^+$–$\tilde{X}\,^2\Pi_i$) system obtained by electron impact on jet-cooled N_2O at 100 eV; the optical resolution is 0.05 nm (FWHM).

TABLE I. Relative band strengths of the $N_2O^+(\tilde{A}\ ^2\Sigma^+,\ v'\text{–}\tilde{X}\ ^2\Pi,\ v'')$ emission measured at an impact energy of 100 eV.[a]

$v''\backslash v'$	0^0	1^1	1^2	2^1K^1	2^2K^0	3^1
0_0	100 (100)	13.3(14.4)		0.5		
1_1	50.7(57.2)	5.5 (8.2)	0.4			
1_2	15.6(15.5)	9.6 (9.5)				
1_3	2.6 (2.6)	6.4 (5.8)	0.7			
1_4	0.7 (1.1)	1.4 (1.5)				
2_1K_0	4.1 (9.6)	1.1		5.0		
2_1K_2				5.3		
$1_12_1K_0$	2.2			2.8		
$1_12_1K_2$				4.3		
2_2K_1	3.2			1.1	1.4 (0.9)	
3_1	2.0 (2.1)	2.7				6.6 (6.4)
1_13_1	1.8 (1.8)	1.6				3.3
1_23_1	1.2	1.3				1.6

[a] Numbers in parentheses are evaluated from the emission cross sections measured by Sprang *et al.*; Ref. 3.

tative data on the dependence of R_e on $\bar{r}$. The difficulty in such a measurement is probably caused by predissociation of higher vibrational levels of the $\tilde{A}$ state. In the present analysis, the transition moment is assumed to be invariant with the internuclear distance. Thus, from Eq. (1), it is apparent that the band strengths,[21] $I(v',\ v'')/\nu(v',\ v'')^3$, are proportional to the FCFs among the same upper level. The relative band strengths thus obtained are listed in Table I and compared with the electron impact data of Sprang *et al.*[3]

To our knowledge, there is no complete data on the FCF for the $N_2O^+(\tilde{A}\text{–}\tilde{X})$ system. Therefore, the method employed by Endoh *et al.*[22] was applied in order to determine vibrational distributions of the $\tilde{A}$ state. Since the summation of $q(v', v'')$ over all v'' values is equal to one, Eq. (1) reduces to

$$N(v') \propto \frac{1}{\Phi_F(v')} \sum_{v''} \frac{I(v',v'')}{\nu(v',v'')^3}. \qquad (2)$$

The approximation of R_e = constant spoils very little the population analysis because of the summation in Eq. (2).[3] Thus, if all of the vibrational bands are isolated, Eq. (2) is applicable to the population analysis. Any effects due to the anisotropy of fluorescence are neglected; in fact, the polarization for the $N_2O^+(\tilde{A}\text{–}\tilde{X})$ emission is expected to be rather small since the fluorescence transition moment is perpendicular to the molecular axis.[7]

The vibrational populations of the six vibrational levels of the $\tilde{A}$ state were evaluated from fluorescence intensities of the 32 bands in the 335–422 nm region; besides, no emission was recognized in the other regions. The obtained values were corrected for the fluorescence quantum yield Φ_F. On the basis of the published data on the fluorescence quantum yields,[5,19,23–25] we have assumed that $\Phi_F(0^0) = 1.0$, $\Phi_F(2^1) = 0.8$, $\Phi_F(2^2K^0) = 0.25$, $\Phi_F(1^1) = 0.7$, $\Phi_F(1^2) = 0.5$, and $\Phi_F(3^1) = 0.6$. Determination of the Φ_F values for the six levels will be discussed below. Table II summarizes the relative vibrational populations of the $\tilde{A}$ state produced in the impact energy range of 22–100 eV comparing with the data obtained from electron-impact optical spectroscopy (EI),[3] photoelectron spectroscopy (PES, TPES),[4–6] and Penning ionization optical spectroscopy (PIOS).[26] The data are also compared with the values derived from the theoretical FCFs for the $N_2O^+(\tilde{A})\text{–}N_2O(\tilde{X})$ system.[27,28]

C. Franck–Condon factors

The band strengths with the same upper level (listed in Table I) are taken to be proportional to the FCFs. There is however very little data on the theoretical FCFs for the $N_2O^+(\tilde{A}\ ^2\Sigma^+\text{–}\tilde{X}\ ^2\Pi)$ system. Thus, the FCFs have been calculated in order to compare with the observed values. The normal coordinates of N_2O^+ generally involve simultaneous changes in both N–N and N–O bond lengths and the relative contribution of each displacement coordinate depends on the force field. For such triatomic molecules, the

TABLE II. Relative vibrational populations $N(v')$ of the $N_2O^+(\tilde{A},\ v')$ state.[a]

Method[b]	Reference	Impact energy (eV)	Vibrational level								
			0^0	2^1K^1	2^2K^0	1^1	$1^12^1K^1$	3^1	1^2	1^13^1	3^2
EI	This work	22	58.1(11)	9.4(4)	2.2(4)	22.4(10)		6.4(8)	1.2(2)		
		26	60.5(10)	10.0(4)	1.7(2)	21.1(10)		5.6(8)	1.1(2)		
		30	60.2(9)	9.5(2)	1.8(2)	21.3(6)		6.1(6)	1.1(2)		
		100	60.9(8)	9.2(2)	1.9(2)	20.4(6)		6.8(6)	0.8(2)		
EI	Ref. 3	100	72.1		1.4	22.1	0.4	4.0			
PES	Ref. 4	21.2	74.9	0.2		16.4	0.8	7.3			0.4
PES	Ref. 6	21.2	73.7	1.5		16.0	0.8	6.3	0.3	0.7	0.4
TPES	Ref. 5	SR[c]	62.3			24.6		6.7	4.5		
PIOS	Ref. 26	19.8	68.8	2.6		21.0		7.2	0.5		
FCF	Ref. 27		63			19.6		8.2	3.4	2.6	0.9
FCF	Ref. 28		75.7		0.0	16.4		6.4	0.5	0.0	0.5

[a] Numbers in parentheses in this work mean twice the standard deviation attached to the last digit.
[b] Electron-impact optical spectroscopy (EI), photoelectron spectroscopy (PES), threshold photoelectron spectroscopy (TPES), Penning ionization optical spectroscopy (PIOS), and FCFs calculated for the $N_2O^+(\tilde{A},\ v')\text{–}N_2O(\tilde{X},\ v''=0)$ system; the EI and PIOS data are corrected for Φ_F (see text).
[c] Synchrotron radiation.

TABLE III. Parameters of N_2O^+ and N_2O used for FCF calculations (in cm^{-1} and pm).[a]

	$\tilde{X}\,^2\Pi$	$\tilde{A}\,^2\Sigma^+$	$\tilde{X}\,^1\Sigma^+$
ω_1	1148.0	1355.7	
ωx_1	12.88	5.1[b]	
ω_2		614.1	588.8
r_{NN}	115.5(9)	114.0(6)	112.9
r_{NO}	118.5(9)	114.2(6)	119.1

[a] Adopted from Ref. 17.
[b] Estimated from the transition frequencies of the 0_0^0, 1_1^1, and 1_1^2 bands given by Callomon and Creutzberg.

TABLE IV. Comparison of the relative populations for the bending vibration of the N_2O^+ $(\tilde{A}, v')$ state.

	v'		
Method	0^0	2^1K^1	2^2K^0
Electron impact[a]	100	9.5 ± 0.6	1.9 ± 0.3
Calculation[b]	100	7.7	0.3

[a] An average in the impact energy of 22–100 eV.
[b] FCFs calculated on the assumption of the $D_{\infty h}$ symmetry and a harmonic oscillator function.

method of Coon *et al.*[29] and the generation function method[30] are usually adopted in FCF calculations. In the present study, however, the interaction force constants were ignored. In this simple model the potential function can be reduced to a set of one-dimensional oscillators.

In the observed band strengths, the ν_1 progressions are complete, whereas the ν_2 and ν_3 progressions are incomplete. Thus, the FCFs only for the symmetric stretching (ν_1) were calculated. Moreover, the $D_{\infty h}$ symmetry was assumed since the N–N bond length is nearly equal to the N–O bond length in both states; namely, the reduced mass and the normal coordinate for the symmetric stretching were approximated to be $m_N m_O/(m_N + m_O)$ and $(r_{NN} + r_{NO})/\sqrt{2}$, respectively. The molecular parameters adopted from Callomon and Creutzberg[17] are listed in Table III. The agreement was improved with the introduction of the Morse oscillator potential function. The FCFs calculated by use of the Morse oscillator function are compared with the observed band intensities of the 1^0 and 1^1 progressions in Fig. 2.

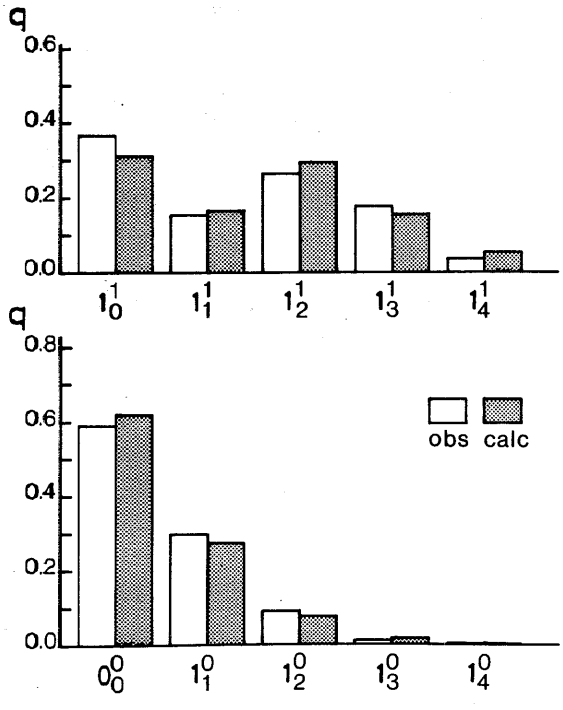

FIG. 2. Relative band intensities of the 1^0 and 1^1 progressions for the N_2O^+ $(\tilde{A}$–$\tilde{X})$ transition.

The vibrational populations $N(v')$ of the $\tilde{A}$ state corrected for predissociation should be proportional to the theoretical FCFs for the $N_2O^+(\tilde{A}, v')$–$N_2O(\tilde{X}, v'' = 0)$ system. The FCF values calculated by Rosenstock[27] could not reproduce the observed data,[4] whereas those calculated by Chau[28] are in good agreement with the observed data.[6] Unfortunately, Rosenstock[27] did not treat the bending vibration and Chau[28] did not list the FCF value for the 2_0^1 band as shown in Table II. Therefore, the FCFs of the bending vibration are calculated in order to compare with the observed populations of the 2^1K^1 and 2^2K^0 levels. In the calculations, the $D_{\infty h}$ symmetry and a harmonic oscillator were assumed for the potential of the bending vibration; namely, the reduced mass was approximated by $m_N(m_N + m_O)/(8m_N + 4m_O)$ and the normal coordinate was represented by $(r_{NN} + r_{NO})\phi_{NNO}/2$. The ν_2 frequency and the bond lengths[17] are listed in Table III. Table IV shows the relative populations for the bending vibration calculated from the FCFs on comparing with the observed values.

IV. DISCUSSION

Sprang *et al.*[3] have measured the emission cross sections for several vibrational bands of the N_2O^+ $(\tilde{A}$–$\tilde{X})$ system at 100 eV. The band strengths evaluated from their emission cross sections are however fairly different from the present results as shown in Table I. This discrepancy is probably due to either the incompleteness of their data on the emission cross section or the lower resolution in their experiments.

Figure 2 shows the observed band intensities of the 1^0 and 1^1 progressions comparing with the FCFs for the N_2O^+ $(\tilde{A}$–$\tilde{X})$ system calculated by the simple method as described in Sec. III C. The observed values of both progressions almost agree with the calculated FCFs. The agreement achieved by this simple calculation will provide information for more detailed studies on the FCF calculation for the N_2O^+ $(\tilde{A}$–$\tilde{X})$ system.

In the present study the $N(v')$ values represent the nascent vibrational distribution of the $\tilde{A}$ state if (i) collisional relaxation, (ii) cascading from upper ion states, and (iii) predissociation can be ignored.

(i) *Collisional relaxation:* The frequency of collisions that an N_2O^+ $(\tilde{A}, v')$ suffers in the free jet expansion under

our experimental conditions is estimated to be about 6×10^3 s^{-1} from the theoretical data obtained by Lubman *et al.*[31] on the assumption of a quenching cross section of 3 Å^2.[32] Thus, the collisional probability during the lifetime is in the order of 10^{-4} on comparing with the fluorescence lifetimes of the 0^0, 1^1, and 3^1 levels, 180–260 ns.[3,24,25,32] Hence, collisional relaxations are negligible.

(ii) *Cascading from upper ion states:* Electron-impact ionization at impact energies above 20 eV can produce the $\tilde{B}\,^2\Pi$ and $\tilde{C}\,^2\Sigma^+$ states[33] in addition to the $\tilde{A}$ state. However, these higher lying ionic states completely predissociate,[34] so that the radiative cascading from these states to the $\tilde{A}$ state is insignificant.

(iii) *Predissociation:* In the HeI photoelectron–photoion coincidence measurement,[19] Eland pointed out that N_2O^+ ions in the 0^0 level of the $\tilde{A}$ state all fluoresce, whereas about 40% of the ions in the 1^1, 1^2, and 3^1 levels predissociate. These results agree well with the values inferred from the photodissociation quantum yields.[35] In contrast, combining photoelectron and photofluorescence data, Lee[36] pointed out that the contribution of predissociation of the 1^1 level must be small. On the basis of Lee's result and the lifetime data, Sprang *et al.*[3] concluded that the predissociation ratio given by Eland[19] is probably 2–3 times too high. Thus, the reported Φ_F values were not always consistent each other. Since then, the data of fluorescence quantum yields have been accumulated by several methods such as photoelectron–photoion coincidence,[23] photoelectron–photon coincidence,[5,24] and fluorescence decay[25,32] and then the reported values are consistent with Eland's data. Therefore, the Φ_F values seem to be established at present.

In the present study an average of the published data for each level[5,19,23–25,32] has been adopted as the Φ_F value. The uncertainties in the Φ_F values, which are described in Sec. III B, are estimated to be 4% for the 0^0 level ($\Phi_F = 1.0$) and 10% of the given value for the other five levels according to the quoted uncertainties. Nevertheless, the determination of the vibrational populations of the $\tilde{A}$ state depends critically on the Φ_F value for each level. Even if the Φ_F values are revised, one can easily correct the populations of the six levels listed in Table II. We do not mention the Φ_F values for the remaining $1^12^1K^1$, 1^13^1, and 3^2 levels which are not observed in the present study.

Therefore, it is concluded that the observed vibrational populations corrected for predissociation are very close to those for the nascent $\tilde{A}$ ion state. The experimental uncertainties shown in Table II include variations in the emission intensity for various experimental spectra, errors arising from overlapping bands, and errors in the calibration of the efficiency of the fluorescence detecting system. The uncertainty in the intensity calibration is estimated to be 4%.

The branching ratios of $N(1^1)/N(0^0)$ and $N(3^1)/N(0^0)$ derived from the values in Table II should be equal to the $\sigma(1^1)/\sigma(0^0)$ and $\sigma(3^1)/\sigma(0^0)$ ratios, respectively, of the previous study.[14] The value of $N(1^1)/N(0^0)$, 0.335(11), obtained at 100 eV however is apparently larger than the $\sigma(1^1)/\sigma(0^0)$ ratio of 0.253(8). In the previous study, the branching ratio was evaluated by applying Eq. (1) to both the 0_0^0 and the 1_0^1 bands. In this case, the ratio of $N(1^1)/N(0^0)$ is given by

$$\frac{N(1^1)}{N(0^0)} = \frac{I(1_0^1)/\nu(1_0^1)^3}{I(0_0^0)/\nu(0_0^0)^3}\cdot\frac{\Phi_F(0^0)q(0_0^0)}{\Phi_F(1^1)q(1_0^1)},$$

where the emission intensities are represented by the heights of peaks. The ratio of the band strength thus obtained agrees precisely with the present ratio (Table I), where the areas under the bands are used as the emission intensities. Therefore, we have concluded that the discrepancy in the branching ratio is caused by the ratio of $\Phi(1^1)q(1_0^1)/\Phi(0^0)q(0_0^0)$ used in the previous calculation. By using the FCFs, $q(0_0^0) = 0.621$ and $q(1_0^1) = 0.311$, calculated in the present study and $\Phi(1^1)/\Phi(0^0) = 0.7$, the ratio of $q(1_0^1)\Phi(1^1)/q(0_0^0)\Phi(0^0)$ is evaluated to be 0.351, which is remarkably smaller than the previous value of 0.553. The $N(1_0^1)/N(0_0^0)$ ratio reevaluated is 0.379(8). When the uncertainties in the FCFs and the fluorescence quantum yields are taken into account, this value is in reasonable agreement with the ratio derived from the values in Table II.

The observed vibrational populations (Table II), particularly for the 2^1K^1, 2^2K^0, 1^1, and 1^2 levels, are fairly different from the PES results[4,6] and the theoretical FCFs $q_{0v'}$ calculated for the $N_2O^+(\tilde{A},\ v')$–$N_2O(\tilde{X},\ v''=0)$ system.[28] These discrepancies are ascribed to two different origins which will be discussed below.

First, the populations of the 1^1 and 1^2 levels are similar to the TPES data[5] rather than the HeI PES data.[4,6] Autoionization of Rydberg states enhances selectively populations of the higher vibrational levels of the $\tilde{A}\,^2\Sigma^+$ state, thus bands, in particular, with the higher quanta of the symmetric stretching become more intense in the TPES than in the PES.[6] In the partial photoionization cross sections for the 0^0, 1^1, and 3^1 levels of the $\tilde{A}$ state obtained by monitoring the fluorescence intensity,[7,8] there are many sharp features assigned to the Rydberg series converging to the $\tilde{C}\,^2\Sigma^+$ state. In the electron-energy-loss spectrum of N_2O using a residual energy of 80 eV,[33] Rydberg series converging to the $\tilde{C}\,^2\Sigma^+$ state are prominent. Accordingly, the enhancement in the populations of the 1^1 and 1^2 levels in the present result compared with the PES data is probably attributed to autoionization of the Rydberg states converging to the $\tilde{C}\,^2\Sigma^+$ state. This conclusion is the same as that described in the previous study.[14]

Second, the population of the 2^1K^1 level is enhanced remarkably more than the PES results.[4,6] The 2^1K^1 level of the $\tilde{A}\,^2\Sigma^+$ ion state has a $^2\Pi$ vibronic symmetry, thus its formation from the ground state of N_2O becomes optically forbidden because of the $\Delta K = 0$ selection rule.[37] In the photoionization, however, the $\Delta K = \pm 1$ bands do occur weakly as a result of a mixing of the $\tilde{X}\,^2\Pi$ and $\tilde{A}\,^2\Sigma^+$ states.[6] Thus, the population of the 2^1K^1 level is small in the PES results. On the other hand, a qualitative clue to the selection rule for the vibronic quantum number K in electron-impact ionization may be provided if one considers how the momentum of the system is partitioned to the product angular momentum.

In the electron impact, formation of

$N_2O^+(\tilde{A}\ ^2\Sigma^+, v')$ from the vibrational ground state of N_2O is given by

$$N_2O(\tilde{X}\ ^1\Sigma^+, v''=0) + e_i \rightarrow N_2O^+(\tilde{A}\ ^2\Sigma^+, v') + e_s + e_e,$$

where, e_i, e_s, and e_e represent the incident, scattered, and ejected electrons, respectively. In this ionization, both the $^1\Sigma^+$ and the $^2\Sigma^+$ states are described by Hund's case (b) since the spin splitting is small.[17] When the electron spin is neglected, the conservation of angular momentum about the internuclear axis is represented by

$$\Lambda_i + l'' = \Lambda_s + \Lambda_e + l',$$

where, $\Lambda_i(h/2\pi)$, $\Lambda_s(h/2\pi)$, and $\Lambda_e(h/2\pi)$ mean the angular momenta about the internuclear axis of the incident, scattered, and ejected electrons, respectively. The l'' $(=0)$ and l' represent the vibrational angular momentums of the parent and produced ion, respectively. Thus, the selection rule for K is given by

$$\Delta K = l' - l'' = \Lambda_i - \Lambda_s - \Lambda_e.$$

To simplify the situation, it seems worth considering the limiting case.

(i) *Limit of high electron energy:* In this case, the dipole Born approximation is valid. The ionizations with $\Delta K = 0$ become dominant in analogy with photoionization.

(ii) *Limit of low electron energy:* When the impact energy decreases to the ionization threshold, the velocity of the scattered and ejected electrons becomes slow and then they are formed solely as s waves $(\Lambda_s = \Lambda_e = 0)$ because of energy conservation, whereas the incident electron can transmit a substantial angular momentum to the system. Consequently, the orbital angular momentum of the incident electron can be converted to the rotational angular momentum; i.e., $\Delta K = \Lambda_i$.

The two cases discussed above should be taken as extreme cases. In the range of the electron energy employed in the present study, i.e., from 6 eV above the threshold to 100 eV, neither of these extreme cases is completely applicable. At such an intermediate energy, the selection rule for K seems to be absent: namely, the transitions with $\Delta K = 0, \pm 1, \ldots$ can occur. These circumstances result in the enhancement of the 2^1K^1 population in the electron impact.

The observed populations for the bending vibration are listed in Table IV on comparing with the FCF values for the $N_2O^+(\tilde{A}, v')$–$N_2O(\tilde{X}, v''=0)$ system calculated by the simple method as described in Sec. III C. The observed values agree substantially with the calculated FCFs. This is consistent with the conclusion that the transitions with $\Delta K = \pm 1$ are allowed in the electron-impact ionization.

V. SUMMARY

Vibrational distributions of the $N_2O^+(\tilde{A}$–$\tilde{X})$ band have been studied by electron-impact ionization of N_2O.

The population of the 2^1K^1 level produced by electron impact is enhanced remarkably more than the PES data.[4,6] From a qualitative consideration to the selection rule, transitions with $\Delta K = \pm 1$ are allowed in electron-impact ionization of N_2O. This is consistent with the result that the population of the 2^1K^1 level corrected for predissociation is in substantial agreement with the FCF value for the $N_2O^+(\tilde{A})$–$N_2O(\tilde{X})$ system. This indicates that the formation of $N_2O^+(\tilde{A})$ in the electron-impact ionization of N_2O is mainly a Franck–Condon type process. A quantitative discussion looks forward to the theoretical FCFs based on a more accurate force field.

A little departure from the theoretical FCF values is however observed in the populations of the 1^1 and 1^2 levels, which are similar to the TPES data[5] rather than the HeI PES data.[4,6] This result is probably attributed to autoionization of the Rydberg states converging to the $\tilde{C}\ ^2\Sigma^+$ state.

ACKNOWLEDGMENT

This study is partly supported by a grant-in-aid from the Ministry of Education, Science, and Culture.

[1] I. D. Latimer and J. W. McConkey, Proc. Phys. Soc. London **86**, 745 (1965).
[2] G. Yu. Gerzanich, V. V. Skubenich, and I. P. Zapesochnyi, Opt. Spectrosc. **41**, 315 (1976).
[3] H. A. van Sprang, G. R. Möhlmann, and F. J. de Heer, Chem. Phys. **33**, 65 (1978).
[4] C. R. Brundle and D. W. Turner, Int. J. Mass Spectrom. Ion Phys. **2**, 195 (1969).
[5] R. Frey, B. Gotchev, W. B. Peatman, H. Pollak, and E. W. Schlag, Chem. Phys. Lett. **54**, 411 (1978).
[6] P. M. Dehmer, J. L. Dehmer, and W. A. Chupka, J. Chem. Phys. **73**, 126 (1980).
[7] E. D. Poliakoff, M.-H. Ho, M. G. White, and G. E. Leroi, Chem. Phys. Lett. **130**, 91 (1986).
[8] E. D. Poliakoff, M.-H. Ho, G. E. Leroi, and M. G. White, J. Chem. Phys. **85**, 5529 (1986).
[9] L. A. Kelly, L. M. Duffy, B. Space, E. D. Poliakoff, P. Roy, S. H. Southworth, and M. G. White, J. Chem. Phys. **90**, 1544 (1989).
[10] T. A. Ferrett, A. C. Parr, S. H. Southworth, J. E. Hardis, and J. L. Dehmer, J. Chem. Phys. **90**, 1551 (1989).
[11] M. Braunstein and V. Mckoy, J. Chem. Phys. **87**, 224 (1987).
[12] M. Braunstein and V. Mckoy, J. Chem. Phys. **90**, 1535 (1989).
[13] J. Berkowitz and J. H. D. Eland, J. Chem. Phys. **67**, 2740 (1977).
[14] H. Kume, H. Shimada, M. Kobayashi, I. Tokue, and Y. Ito, Chem. Phys. Lett. **179**, 109 (1991).
[15] I. Tokue, A. Masuda, H. Kume, and Y. Ito, Chem. Phys. **158**, 161 (1991).
[16] I. Tokue, H. Shimada, A. Masuda, Y. Ito, and H. Kume, J. Chem. Phys. **93**, 4812 (1990).
[17] J. H. Callomon and F. Creutzberg, Philos. Trans. R. Soc. London, Ser. A **277**, 20 (1974).
[18] M. Tsuji, K. Tsuji, and Y. Nishimura, Int. J. Mass Spectrom. Ion Phys. **30**, 175 (1979).
[19] J. H. D. Eland, Int. J. Mass Spectrom. Ion Phys. **12**, 389 (1973).
[20] G. Herzberg, *Molecular Spectra and Molecular Structure I. Spectra of Diatomic Molecules* (Van Nostrand Reinhold, New York, 1950), p. 199.
[21] L. C. Lee and D. L. Judge, J. Phys. B **7**, 626 (1974).
[22] M. Endoh, M. Tsuji, and Y. Nishimura, J. Chem. Phys. **77**, 4027 (1982).
[23] I. Nenner, P-M. Guyon, T. Baer, and T. R. Govers, J. Chem. Phys. **72**, 6587 (1980).
[24] J. P. Maier and F. Thommen, Chem. Phys. **51**, 319 (1980).
[25] D. Klapstein and J. P. Maier, Chem. Phys. Lett. **83**, 590 (1981).
[26] H. Sekiya, M. Endoh, M. Tsuji, and Y. Nishimura, Nippon Kagaku-kaishi **1984**, 1498.
[27] H. M. Rosenstock, Int. J. Mass Spectrom. Ion Phys. **7**, 33 (1971).
[28] F. T. Chau, J. Mol. Struct. **151**, 157 (1987).
[29] J. B. Coon, R. E. DeWames, and C. M. Loyd, J. Mol. Spectrosc. **8**, 235 (1962).
[30] T. E. Sharp and H. M. Rosenstock, J. Chem. Phys. **41**, 3453 (1964).
[31] D. M. Lubman, C. T. Rettner, and R. N. Zare, J. Phys. Chem. **86**, 1129 (1982).
[32] T. Ibuki and N. Sugita, J. Chem. Phys. **80**, 4625 (1984).

[33] K. England, T. Reddish, and J. Comer, Chem. Phys. **119**, 435 (1988).
[34] A. P. Hitchcock, C. E. Brion, and M. J. van der Wiel, Chem. Phys. **45**, 461 (1980).
[35] T. F. Thomas, F. Dale, and J. F. Paulson, J. Chem. Phys. **67**, 793 (1977).
[36] L. C. Lee, J. Phys. B **10**, 3033 (1977).
[37] G. Herzberg, *Molecular Spectra and Molecular Structure III. Electronic Spectra of Polyatomic Molecules* (Van Nostrand, Princeton, 1967), p. 184.